ACS SENSORS

pubs.acs.org/acssensors

Article

Click-Coupling to Electrostatically Grafted Polymers Greatly Improves the Stability of a Continuous Monitoring Sensor with Single-Molecule Resolution

Yu-Ting Lin, Rosan Vermaas, Junhong Yan, Arthur M. de Jong, and Menno W.J. Prins*

Cite This: *ACS Sens.* 2021, 6, 1980−1986

Read Online

ACCESS | Metrics & More | Article Recommendations | Supporting Information

ABSTRACT: Sensing technologies for the real-time monitoring of biomolecules will allow studies of dynamic changes in biological systems and the development of control strategies based on measured responses. Here, we describe a molecular architecture and coupling process that allow continuous measurements of low-concentration biomolecules over long durations in a sensing technology with single-molecule resolution. The sensor is based on measuring temporal changes of the motion of particles upon binding and unbinding of analyte molecules. The biofunctionalization involves covalent coupling by click chemistry to PLL-*g*-PEG bottlebrush polymers. The polymer is grafted to a surface by multivalent electrostatic interactions, while the poly(ethylene glycol) suppresses nonspecific binding of biomolecules. With this biofunctionalization strategy, we demonstrate the continuous monitoring of single-stranded DNA and a medically relevant small-molecule analyte (creatinine), in sandwich and competitive assays, in buffer and in filtered blood plasma, with picomolar, nanomolar, and micromolar analyte concentrations, and with continuous sensor operation over 10 h.

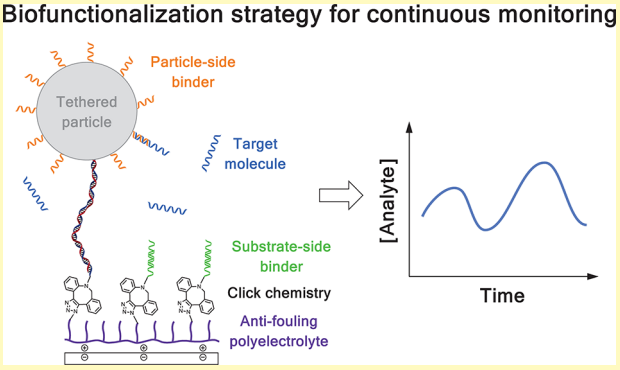

KEYWORDS: *continuous monitoring biosensors, biofunctionalization, low-fouling, polyelectrolyte, click chemistry*

Biological systems exhibit dynamics that are at the most basic level driven by time-dependent changes of molecules such as metabolites, hormones, proteins, and nucleic acids. For healthcare and engineering purposes, it would be highly valuable to be able to continuously monitor specific molecules that critically reflect the biological dynamics so that timely actions can be taken and changes can be managed. A good example is sensors for continuous glucose monitoring, which are used for patient self-monitoring[1] as well as for controlling industrial fermentations and bioreactors.[2]

Glucose is a metabolite that is present at millimolar concentrations. Biomarkers at lower concentrations can be measured with well-established detection techniques such as surface plasmon resonance (SPR), quartz crystal microbalance (QCM), and enzyme-linked immunosorbent assays (ELISA). However, these methods involve fluid handling steps (e.g., washing steps), which complicate the design of a monitoring system. A sensing principle that does not require wash steps is electrochemical aptamer-based sensing, based on analyte-induced conformational changes of surface-coupled aptamers.[3] Research groups have demonstrated the monitoring of micromolar and nanomolar analyte concentrations.[4−6] However, the continuous monitoring of biomarkers in the picomolar concentration range has not come within reach.

We have recently demonstrated a sensing technology for continuous biomarker monitoring at micromolar, nanomolar, and picomolar concentrations, called biosensing by particle mobility (BPM).[7−9] The BPM sensing method has single-molecule resolution and gives digital signals, which enables measurements at low concentrations.[10] BPM is based on particles tethered to a substrate, where the particles and the substrate are functionalized with specific binder molecules. Temporal changes are detected in the mobility of the particles caused by the reversible binding and unbinding of analyte molecules, generating digital on−off switching related to single-molecule events. The BPM sensing principle has been demonstrated with oligonucleotides and proteins as binder molecules, for sensing DNA, protein, as well as small-molecule biomarkers. However, the reported data show a decay of sensor signals, limiting the duration of the experiments as well as the duration of sensor operation in prospective applications.

Received: March 18, 2021
Accepted: April 29, 2021
Published: May 14, 2021

https://doi.org/10.1021/acssensors.1c00564
ACS Sens. 2021, 6, 1980−1986

Potential causes of the signal decay are imperfect blocking strategies and a loss of binder molecules over time due to noncovalent coupling methods.

In this paper, we describe a molecular architecture with low-fouling bottlebrush polymers (PLL-*g*-PEG)[11] and covalent click-coupling[12,13] for achieving real-time continuous monitoring of analytes at low concentrations with stable response over long durations. The bottlebrush polymer serves four purposes: (i) it is strongly attached to the substrate by multivalent electrostatic interactions for high sensor stability, (ii) polyethylene glycol groups give low-fouling properties[14,15] in order to reduce nonspecific binding of biomolecules, (iii) the polymer serves as a spacer between binder molecules and the solid substrate for minimizing loss of biomolecular activity over time, and (iv) integrated click-functional groups allow facile covalent coupling of binder molecules.

We show that the molecular architecture with click-coupling to low-fouling polymers greatly improves the stability of the BPM continuous monitoring sensor with single-molecule resolution. We describe the molecular architecture, compare it to previous coupling methods, and demonstrate the continuous monitoring of single-stranded DNA (ssDNA) and a small-molecule analyte (creatinine), in sandwich and competitive assay formats, in buffer and in filtered blood plasma. Picomolar, nanomolar, and micromolar analyte concentrations are measured with continuous sensor operation over long durations.

RESULTS

Sensing Approach. Biosensing by particle mobility (BPM) is based on particles that are tethered to a substrate via double-stranded DNA (dsDNA), with the particles and the substrate coated with binder molecules such as oligonucleotides or antibodies.[7,9] The particles show Brownian motion and explore a region related to the length of the dsDNA tether. In a sandwich assay format (see Figure 1), target molecules can simultaneously bind to a binder molecule on the particle (particle-side binder, also referred to as "particle binder") and a binder molecule on the substrate (substrate-side binder, also referred to as "substrate binder"). The formation of a target-induced sandwich bond between the particle and the substrate causes the particle motion to become more restricted (bound state), which can optically be detected. Upon dissociation of the target molecule, the larger motion amplitude of the particle is restored (unbound state). The increase and decrease in particle motion, as a result of binding and unbinding of target molecules, are detected over time.[7] The output of the BPM biosensor is the particle switching activity, defined as the average frequency of binding and unbinding events per particle, which can be quantitatively related to the target concentration. The sensing principle is reversible and does not consume or produce any reagents, making it highly suited for continuous monitoring over long durations. However, operation over long durations requires a high stability of the biofunctionalizations in the system, which is the topic of this study.

Results and Discussion. The design of the molecular architecture and the particle-based biosensor are shown in Figure 1. A mixture of cationic PLL-*g*-PEG and PLL-*g*-PEG-N_3 polymers is adsorbed onto the negatively charged glass substrate. The polyethylene glycol (PEG) groups are strongly hydrophilic and provide biofouling-resistant properties, used here to reduce nonspecific interactions between particles, the

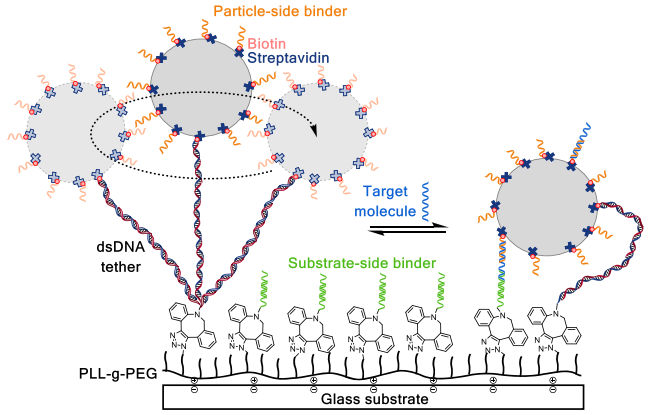

Figure 1. Schematic overview of biosensing by particle mobility (BPM) using click-coupling to a low-fouling bottlebrush polymer, exemplified by a sandwich assay for detecting ssDNA target molecules (not to scale). The substrate is coated with PLL-*g*-PEG-N_3 molecules, for antifouling properties and for click-coupling of DBCO-tagged double-stranded DNA tether molecules (red-blue). The particles and the substrate are provided with binders that have a specific affinity to the target molecule. Target molecules (blue) hybridize with the complementary particle and substrate binders, forming a sandwich arrangement (right). The formed sandwich bond leads to a restriction of the motion of the particle. Due to the reversible affinity interactions, the particle switches between the unbound state (left) and the bound state (right). The switching frequency depends on the target concentration: the frequency is low for low target concentration, and the frequency is high for high target concentration.

substrate, and matrix components. The dsDNA tether and the substrate-side binder molecules are coupled to the PLL-*g*-PEG layer via the integrated azide groups, using second-generation click chemistry that is copper-free, catalyst-free, specific, and biocompatible.[16−19] The surface density of clickable azide groups was controlled by mixing PLL-*g*-PEG and PLL-*g*-PEG-N_3 polymers at a 10:1 ratio. This provides a sufficient number of azide groups on the surface while still enabling a low degree of nonspecific binding. The single tethering of particles was created by coupling DBCO-dsDNA-biotin tethers to the azide groups and thereafter exposing the surface to particles functionalized with streptavidin moieties.

The stability of the tethered particles was characterized by measuring the number of tethered particles over time. Figure 2 shows the percentage of particles that remain tethered to the surface over a 24 h monitoring period. In the reference experiment, the dsDNA tethers were provided with digoxigenin tags and coupled to the substrate using antidigoxigenin antibodies (see our earlier work[7]). The observed time profiles of the two coupling methods are fitted with single-exponential decay curves. The curves show that the click-based coupling is much more stable than the antibody−antigen-based coupling: the rate of particle loss is about 50 times slower for the click-based coupling.

For the click-based coupling, the loss of particles over a period of 24 h is about 20%. Possible origins of the observed loss are the detachment of the PLL-*g*-PEG layer from the glass substrate, the breaking of the DBCO−azide bond, or the dissociation of the biotin−streptavidin bond on the particle. The dissociation rate of biotin−streptavidin is about $(5.5 \pm 2.2) \times 10^{-6}$ s^{-1},[20] which is very close to the rate observed in Figure 2. The DBCO−azide conjugate, formed through click chemistry, has been proven to be stable under a pulling force of

https://doi.org/10.1021/acssensors.1c00564
ACS Sens. 2021, 6, 1980−1986

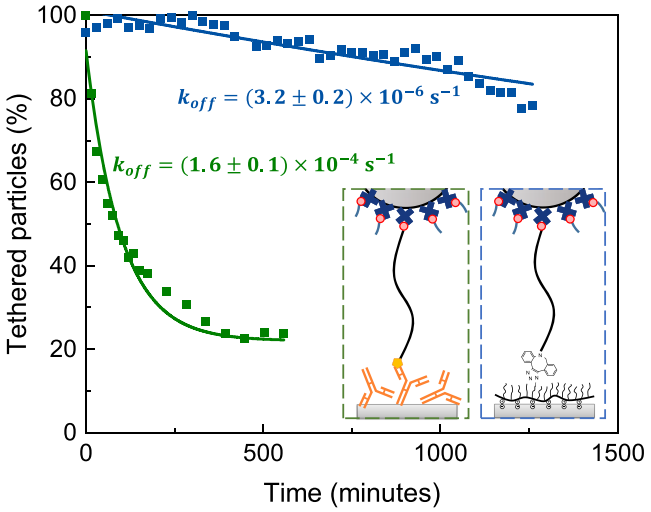

Figure 2. Number of tethered particles measured over time, for two methods of coupling the dsDNA tether to the substrate: DIG-AntiDIG coupling (green) and click chemistry (blue). The fluid cell was turned over so that dissociated particles sediment and move away from the glass substrate. The curves were normalized at $t = 0$ and have been fitted with an exponential decay function: $f(t) = (1 - a) + a \times \exp(-t \cdot k_{off})$, with $f(t)$ the fraction of particles bound to the substrate as a function of time, k_{off} the dissociation rate constant of single-tethered particles, a the initial fraction of single-tethered particles, and $(1 - a)$ the initial fraction of particles that are strongly bound, i.e., double-tethered or nonspecifically bound. The fitted k_{off} values are indicated at the curves. The initial number of particles in the experiments was around 500. Negative control experiments are discussed in Supporting Information Section 2.

150 pN for more than 24 h.[17,21] The strength of the PLL-*g*-PEG coupling to the glass substrate is dependent on the surface charge density of the substrate; studies have shown that PLL-*g*-PEG-modified surfaces stay passivated over days.[22−25] Therefore, the loss rate of particles in the PLL-*g*-PEG experiment in Figure 2 is most likely caused by the dissociation of biotin−streptavidin bonds between the biotinylated dsDNA tether and the streptavidin-functionalized particle.

The reversibility of the BPM sensor with click-based coupling is studied in Figure 3, for a DNA sandwich assay as sketched in Figure 1. The particles and the substrate are provided with ssDNA molecules having 10-bp and 9-bp complementarity to the ssDNA target, respectively, resulting in a bound state lifetime in the order of seconds. Figure 3a shows the applied concentration profile (top panel) and the measured switching activity (bottom panel). The switching activity is the frequency of binding and unbinding events observed per particle, averaged over the number of tethered particles in the microscopic field of view and over a measurement duration of 5 min. Typically, a few hundred particles are simultaneously imaged and tracked. The averaging makes the switching activity a normalized parameter that is independent of the number of observed particles. The total number of particles is important for achieving good event statistics and small error bars in the measured switching activity parameter. Measurements with less particles give lower numbers of switching events and therefore larger measurement uncertainties due to lower event statistics. We typically have 500 to 1000 particles in one field of view. To achieve a CV of 5%, at least 400 events need to be collected per measurement point.[9]

The switching activity signal in Figure 3a dynamically responds to both increasing and decreasing target concentrations. The activity increases for increasing target concentration, as is expected for a sandwich assay. When the target concentration is decreased to zero in a single step, the activity drops with a finite response time. The three measured step responses are fitted with exponential decay curves, see the gray lines, showing that the dynamic response can be described with a single time constant τ_{off} of 26.5 ± 2.0 min. The fitted τ_{off} values of the three subsequent step responses are equal within their uncertainty intervals, demonstrating that the time constant is independent of analyte concentration. This implies that the binding between the particles and the substrate is monovalent and that the relaxation time reflects the single-molecule dissociation constant of the weakest link, i.e., the binding between the target molecule and the substrate binder. Furthermore, the data prove that the sensor system is reversible and stable over a time period of several hours.

Figure 3b shows the data points measured in panel (a) but now plotted as a dose−response graph, i.e., the measured signal as a function of the applied target concentration. The correspondence between the data points in the two panels is highlighted by their colors. Figure 3b shows that the data measured with the click-coupling is consistent over the different time periods. The data is fitted with the Hill equation $A([T]) = A_{bg} + A_a \times \frac{[T]}{EC50 + [T]}$, with A the switching activity, A_{bg} the background activity, A_a the activity amplitude, $[T]$ the target concentration, and EC50 the target concentration at which the response reaches 50% of the activity amplitude. The data show that the sensor response is consistent over a period of 10 h, using the molecular architecture with click-based coupling on a low-fouling polymer.

The PEG side chains of the PLL-*g*-PEG polymer are expected to function as a low-fouling layer that resists protein adsorption. Figure 3c,d shows the response of the BPM sensor in filtered undiluted blood plasma. The data in plasma and in buffer show good correspondence, both in time−response and in dose−response curves, proving that the ssDNA target in the picomolar concentration range can be dynamically monitored in very different solutions over long durations. The low-fouling properties of the PLL-*g*-PEG polymer are also apparent in other parameters: (i) the percentage of nonspecifically bound particles is less than 10% (see Supporting Information Section 2), (ii) the room-temperature shelf-life of the PLL-*g*-PEG surface functionalized with oligonucleotides and dsDNA tethers is at least three months (see Supporting Information Section 3), and (iii) analyte measurements in 10% unfiltered blood plasma can be done over a period of 9 h (see Supporting Information Section 4).

The stability of the click-based BPM sensor is improved relative to that of the antibody-anchoring BPM sensor (Supporting Information Section 5). Under similar conditions, the click-based sensor responds quantitatively to the target in filtered undiluted blood plasma with a signal decay rate of (8.3 ± 1.1) × 10^{-6} s^{-1} (on average, less than 10% signal loss was observed over 5 h), while the antibody-anchored sensor exhibits a higher loss of signal (approximately 50% signal loss was observed over 5 h) with a decay rate of (4.5 ± 0.3) × 10^{-5} s^{-1}.

Sandwich assays are suitable for measuring analytes that have two binding sites since the analyte needs to simultaneously bind to both the particle binder and the

https://doi.org/10.1021/acssensors.1c00564
ACS Sens. 2021, 6, 1980−1986

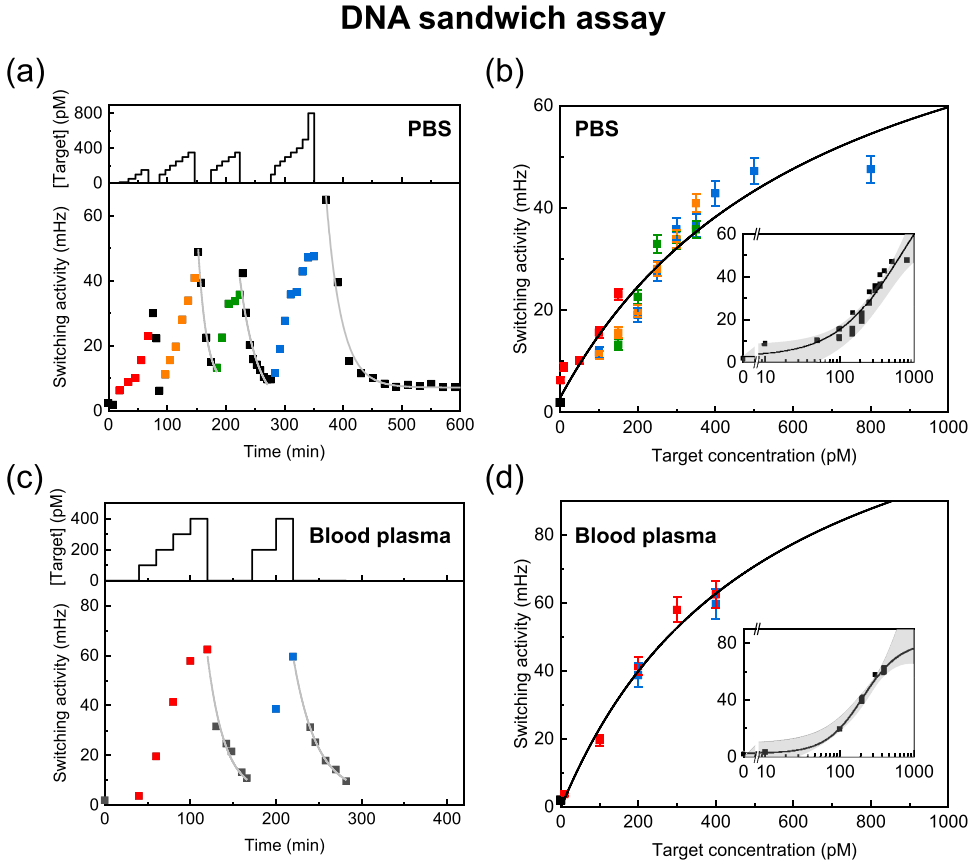

Figure 3. Dynamic response to target concentration of a BPM sensor with click-coupling to the PLL-*g*-PEG polymer, for a DNA sandwich assay in buffer and in filtered undiluted blood plasma. The substrate is functionalized with ssDNA oligonucleotide binders having 9-bp complementarity to the ssDNA target. Particles are provided with ssDNA oligonucleotide binders having 10-bp complementarity. (a) Switching activity measured over time for the ssDNA target in PBS. The top panel shows the concentration−time profile applied to the flow cell. The target concentration was gradually increased in small steps and thereafter returned to zero in a single step; four such profiles were consecutively applied. The bottom panel shows the switching activity of the BPM sensor. The switching activity, defined as the average frequency of binding and unbinding events per particle, shows a positive and reversible response to target concentration. The signal response after application of zero concentration was fitted with a single-exponential decay function (indicated as light gray lines), revealing a time constant of $\tau = 26.5 \pm 2.0$ min. (b) Data of panel (a) plotted in a dose−response graph, i.e., the measured signal as a function of target concentration. The colors of the data points refer to the consecutive concentration−time profiles in panel (a). The inset shows the data with a logarithmic concentration scale. The data points collapse onto a single curve, demonstrating the consistent response and reversibility of the sensor. The data were fitted with the Hill equation $A([T]) = A_{bg} + A_a \times \frac{[T]}{EC50 + [T]}$ (black line), revealing EC50 = 680 ± 268 pM. The measurement errors are the standard errors given by the standard deviation of switching activity divided by the square root of the number of particles.[26] The standard errors show the accuracy of the mean and are strongly dependent on sample size. The gray shade indicates the 95% confidence range of the fit. (c) Switching activity measured for the ssDNA target in 50 kDa spin-filtered bovine blood plasma. The single-exponential decay fits (light gray lines) reveal a time constant of $\tau = 27.0 \pm 2.0$ min. The protein composition of filtered blood plasma was determined with SDS-PAGE, see Supporting Information Section 6. (d) Data of panel (c) plotted in a dose−response graph. The data points collapse onto a single curve with EC50 = 524 ± 257 pM.

substrate binder. For monitoring small molecules with only one binding site, it is necessary to employ a competition assay. Figure 4 shows the sensor design and the sensor response for two competition assays, namely, for monitoring ssDNA and creatinine.[9] Creatinine is a byproduct of muscle metabolism and an important biomarker for monitoring the kidney function.[27] In the competition assays, either the particles or the substrate is provided with molecular binders that compete with the analyte for transient binding of the particles.

In the ssDNA competition assay, the PLL-*g*-PEG surface is covalently functionalized with partially double-stranded substrate binders that function as the analogues (green) with a 9-nt single-stranded binding region pointing outward. Particles are provided with initial biotinylated oligos (gray) having 20-nt complementarity to particle binders (orange). The reversible 9 bp hybridization between substrate binders (ssDNA analogues) and particle binders results in transient switching of particle mobility. In the presence of the 11-nt analyte (blue), the binding region on particle binders is blocked, causing a decrease in switching events. In the creatinine assay, the PLL-*g*-PEG surface is covalently functionalized with substrate binders (gray) having 20-nt complementarity to ssDNA−creatinine conjugates that function in the assay as the analogues (green). Particles are functionalized with anticreatinine antibodies (orange) by biotin−streptavidin coupling. In the absence of the creatinine analyte, the reversible binding of creatinine antibodies to analogues results in switching of particles. When the creatinine analyte is present in solution, then the binding sites on the anticreatinine antibodies are blocked by the analyte, and the switching events of the particles are reduced. For a detailed explanation of the

https://doi.org/10.1021/acssensors.1c00564
ACS Sens. 2021, 6, 1980−1986

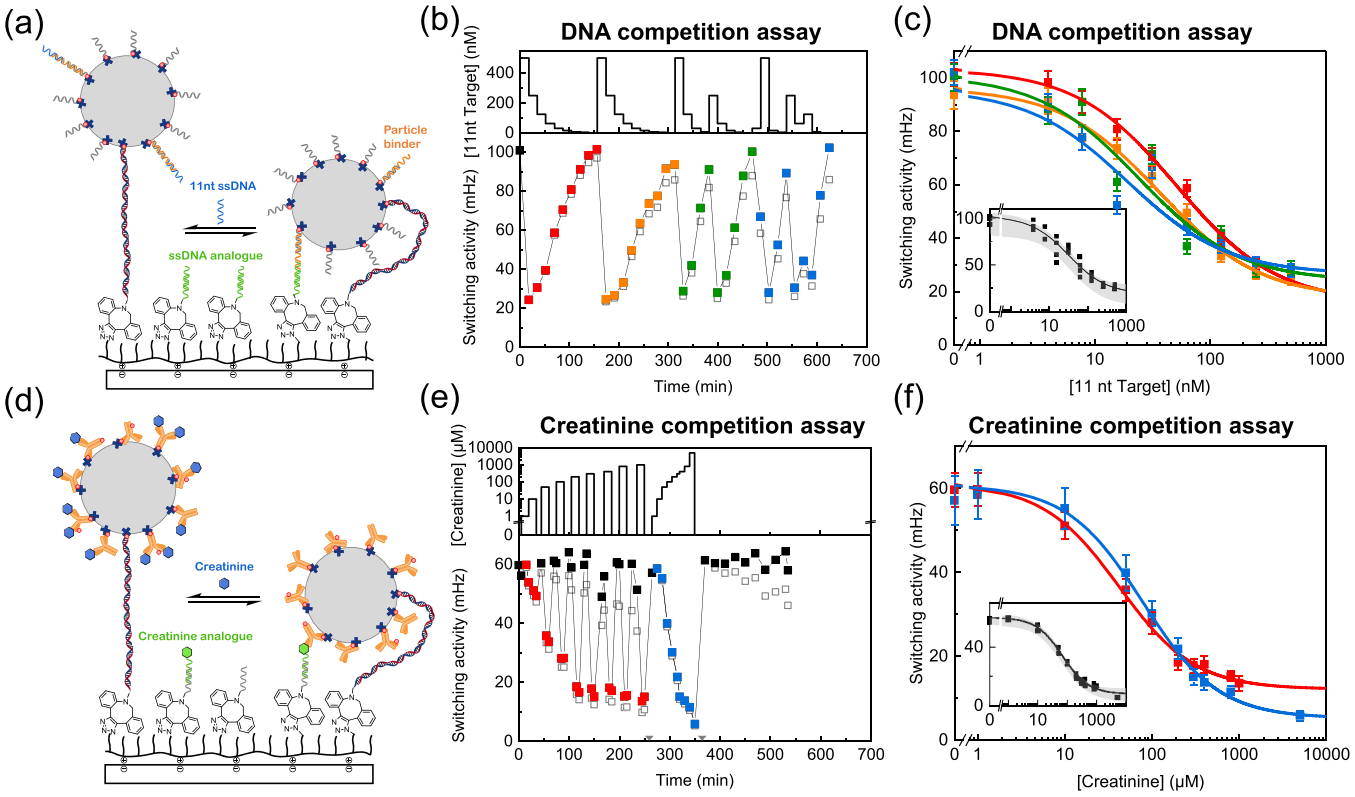

Figure 4. BPM competition assays on the low-fouling PLL-*g*-PEG polymer, for measuring ssDNA (a–c) and creatinine (d–f) in PBS. (a) Schematic drawing of ssDNA competition assay (molecules are not to scale). (b) Switching activity measured over time for the ssDNA target. The top panel shows the concentration–time profiles, and the bottom panel shows the measured switching activity. The switching activity shows an inverted response (high analyte concentration gives low switching activity), as expected for a competition assay. The open squares show the uncorrected data, and the solid squares show the signal corrected for loss; the correction method is described in Supporting Information Section 7. Red and orange data points represent equal decreasing concentration series; green and blue data points represent sequences of alternating concentration values. Lines are guides to the eyes. (c) Dose–response graph containing all data points of panel (b). The data were fitted with the Hill equation (colored lines). The fitted EC50 values are 51 ± 6 nM (red), 37 ± 8 nM (orange), 24 ± 17 nM (green), and 19 ± 13 nM (blue). Small variations in flow conditions within experiments and incomplete exchange of fluids cause small differences in the measured EC50 values. The inset shows the Hill equation fit through all data points simultaneously, with an EC50 of 35 ± 9 nM. The measurement errors are the standard errors of the mean, given by the standard deviation of switching activity divided by the square root of the number of particles.[26] Lines are guides to the eyes. (d) Schematic drawing of creatinine competition assay (molecules are not to scale). (e) Competitive BPM assay with the creatinine analogue on the substrate and the anticreatinine antibody on the particle. The colored squares show the signal corrected for signal loss. The open squares represent the uncorrected data. Two gray triangles on the *x*-axis mark the time points when a chemical reactivation process was applied. The correction method and the reactivation process are described in Supporting Information Section 8. Lines are guides to the eyes. (f) Dose–response graph containing all data points of panel (e). Dose–response curves for the two time periods (red and blue) were separately fitted with the Hill equation. The fitted EC50 values are 42 ± 6 μM (red) and 78 ± 9 μM (blue). The inset shows the Hill equation fit through all data points simultaneously, with an EC50 of 66 ± 8 μM.

competition assays, see Supporting Information Sections 7 and 8.

The data in Figure 4 show reversible sensor responses over long durations for the two very different molecular systems, namely, the competitive oligonucleotide assay (panels (a)–(c)) and the competitive small-molecule immunoassay (panels (d)–(f)). The time-dependent data in Figure 4b,e show that the signal dynamically responds to repeated increases as well as decreases in analyte concentration, applied over a time period of many hours. Compared to the sandwich assays, three interesting differences are seen. First, the competition assays give a sensor with inverted response: an increase in analyte concentration causes a decrease in switching activity because the analyte molecules compete with the analogues. Second, the responses in the competition assays are much faster than the responses in the sandwich assays. The faster response is caused by the law of mass action, as the analyte concentrations are higher in the competition assays compared to the sandwich assays. Third, the competition assays are prepared with a reduced density of binders on the particle side or on the substrate side. A low density is essential in order to achieve reversible monovalent bonds and avoid irreversible multivalent bonds between the particles and the substrate. The density of binders is approximately three orders of magnitude lower in the competition assays compared to the sandwich assay. The open squares in Figure 4b show the raw data of the DNA competition assay. The observed signal decrease follows a straight line with a loss rate of 6×10^{-6} s^{-1} (see Supporting Information Section 7). This rate is equal to the dissociation rate constant of the biotin–streptavidin bonds that are involved in the coupling of the particle-side binders (see Figure 4a). A similar time-dependent dissociation of particle-side binders may have occurred in the sandwich assay experiment of Figure 3, but in that data, the dissociation is not visible due to the small loss of signal compared to the error bars. The predictable nature of the signal loss allows the

https://doi.org/10.1021/acssensors.1c00564
ACS Sens. 2021, 6, 1980–1986

application of a mathematical correction method. The solid data points in Figure 4b represent the measured signal after correction for the loss (see Supporting Information Section 7). The resulting dose−response curves are shown in Figure 4c.

In the creatinine assay, a signal loss rate of 2×10^{-5} s^{-1} is observed (see Supporting Information Section 8). Since proteins are generally less stable than oligonucleotides, the higher loss rate is potentially caused by a gradual loss of activity of the antibodies. Again, the observed rate of signal loss allows the application of a mathematical correction. The solid data points in Figure 4e represent the measured signal after correction for the loss (see Supporting Information Section 8). Alternatively, the original signal can be recovered by supplementing fresh analogues into the flow cell (see experimental results in Supporting Information Section 8). In summary, Figure 4 shows consistent time-dependent responses and dose−response curves, for two very different competition assays (ssDNA oligonucleotide assay and small-molecule immunoassay), over a wide concentration range (nM to mM), over monitoring periods of many hours.

CONCLUSIONS

We have described a biofunctionalization strategy based on click-coupling to a low-fouling polymer for improving the control and durability of real-time continuous biosensing with single-molecule resolution. The bottlebrush polymer (PLL-*g*-PEG) is strongly attached to the substrate by multivalent electrostatic interactions and serves as a spacer between immobilized molecules and the solid substrate. Reversible and consistent responses were observed over long durations in different molecular systems, namely, a sandwich oligonucleotide assay, a competitive oligonucleotide assay, and a competitive small-molecule immunoassay, showing the general applicability of the approach. Picomolar, nanomolar, and micromolar analyte concentrations were measured with continuous sensor operation over many hours. The presented molecular architecture is suited for a variety of substrates and for further industrialization. We found that the shelf-life of the modified surface in a wet state is several months (Supporting Information Section 3). We expect that the sensor with this novel biofunctionalization strategy will enable real-time monitoring for a wide range of applications that can benefit from series of biochemical data and dynamic process control, including biological research as well as medical, pharmaceutical, and industrial applications.

ASSOCIATED CONTENT

Supporting Information

The Supporting Information is available free of charge at https://pubs.acs.org/doi/10.1021/acssensors.1c00564.

Materials and methods, negative control experiments for the click-based coupling approach, shelf-life of the biofunctionalized surface, DNA competition assay in 10% blood plasma over long durations, signal decay rate of the click-based and antibody anchoring-based BPM sensor, SDS-PAGE characterization of filtered blood plasma and diluted blood plasma, and correction of signal decay for ssDNA competition assay and creatinine competition assay (PDF)

AUTHOR INFORMATION

Corresponding Author

Menno W.J. Prins − *Department of Applied Physics, Department of Biomedical Engineering, and Institute for Complex Molecular Systems (ICMS), Eindhoven University of Technology, 5600 MB Eindhoven, The Netherlands; Helia BioMonitoring, 5600 MB Eindhoven, The Netherlands;* orcid.org/0000-0002-9788-7298; Email: m.w.j.prins@tue.nl

Authors

Yu-Ting Lin − *Department of Applied Physics, Eindhoven University of Technology, 5600 MB Eindhoven, The Netherlands;* orcid.org/0000-0003-3235-9491

Rosan Vermaas − *Department of Biomedical Engineering, Eindhoven University of Technology, 5600 MB Eindhoven, The Netherlands*

Junhong Yan − *Helia BioMonitoring, 5600 MB Eindhoven, The Netherlands*

Arthur M. de Jong − *Department of Applied Physics and Institute for Complex Molecular Systems (ICMS), Eindhoven University of Technology, 5600 MB Eindhoven, The Netherlands;* orcid.org/0000-0001-6019-7333

Complete contact information is available at: https://pubs.acs.org/10.1021/acssensors.1c00564

Author Contributions

All authors conceived the methodology, measurement system, and experiments. Y.-T.L. and R.V. performed the experiments and the analysis of the data. All authors discussed results, interpreted data, and co-wrote the paper. All authors approved the submitted version of the manuscript.

Notes

The authors declare the following competing financial interest(s): M.P. is listed as one of the inventors on patent application WO/2016/096901 Biosensor based on a tethered particle. J.Y. and M.P. are cofounders of Helia Biomonitoring BV that has a license to the patent. All authors declare no further competing interests.

ACKNOWLEDGMENTS

We thank Human Gesellschaft für Biochemica und Diagnostica mbH for kindly providing the anticreatinine antibody. We thank Max Bergkamp and Emiel Visser for the particle tracking and event detection algorithms. Part of this work was funded by the Dutch Research Council (NWO), section Applied and Engineering Sciences, under grant number 15481. Part of this work was funded by the Safe-N-Medtech H2020 project under grant agreement no. 814607.

REFERENCES

(1) Rodbard, D. Continuous Glucose Monitoring: A Review of Successes, Challenges, and Opportunities. *Diabetes Technol. Ther.* **2016**, *18*, S2-3−S2-13.

(2) Wasalathanthri, D. P.; Rehmann, M. S.; Song, Y.; Gu, Y.; Mi, L.; Shao, C.; Chemmalil, L.; Lee, J.; Ghose, S.; Borys, M. C.; Ding, J.; Li, Z. J. Technology Outlook for Real-Time Quality Attribute and Process Parameter Monitoring in Biopharmaceutical Development—A Review. *Biotechnol. Bioeng.* **2020**, *117*, 3182.

(3) Schoukroun-Barnes, L. R.; Macazo, F. C.; Gutierrez, B.; Lottermoser, J.; Liu, J.; White, R. J. Reagentless, Structure-Switching, Electrochemical Aptamer-Based Sensors. *Annu. Rev. Anal. Chem.* **2016**, *9*, 163−181.

(4) Schoukroun-Barnes, L. R.; Wagan, S.; White, R. J. Enhancing the Analytical Performance of Electrochemical RNA Aptamer-Based Sensors for Sensitive Detection of Aminoglycoside Antibiotics. *Anal. Chem.* **2014**, *86*, 1131−1137.
(5) Mage, P. L.; Ferguson, B. S.; Maliniak, D.; Ploense, K. L.; Kippin, T. E.; Soh, H. T. Closed-Loop Control of Circulating Drug Levels in Live Animals. *Nat. Biomed. Eng.* **2017**, *1*, No. 0070.
(6) Parolo, C.; Idili, A.; Ortega, G.; Csordas, A.; Hsu, A.; Arroyo-Currás, N.; Yang, Q.; Ferguson, B. S.; Wang, J.; Plaxco, K. W. Real-Time Monitoring of a Protein Biomarker. *ACS sensors* **2020**, *5*, 1877.
(7) Visser, E. W. A.; Yan, J.; Van IJzendoorn, L. J.; Prins, M. W. J. Continuous Biomarker Monitoring by Particle Mobility Sensing with Single Molecule Resolution. *Nat. Commun.* **2018**, *9*, 2541−2510.
(8) Lubken, R. M.; De Jong, A. M.; Prins, M. W. J. Multiplexed Continuous Biosensing by Single-Molecule Encoded Nanoswitches. *Nano Lett.* **2020**, *20*, 2296−2302.
(9) Yan, J.; Van Smeden, L.; Merkx, M.; Zijlstra, P.; Prins, M. W. J. Continuous Small-Molecule Monitoring with a Digital Single-Particle Switch. *ACS Sensors* **2020**, *5*, 1168−1176.
(10) Farka, Z.; Mickert, M. J.; Pastucha, M.; Mikušová, Z.; Skládal, P.; Gorris, H. H. Advances in Optical Single-Molecule Detection: En Route to Supersensitive Bioaffinity Assays. *Angew. Chemie - Int. Ed.* **2020**, *59*, 10746−10773.
(11) Vaisocherová, H.; Brynda, E.; Homola, J. Functionalizable Low-Fouling Coatings for Label-Free Biosensing in Complex Biological Media: Advances and Applications. *Anal. Bioanal. Chem.* **2015**, *407*, 3927−3953.
(12) Kim, E.; Koo, H. Biomedical Applications of Copper-Free Click Chemistry: In Vitro, in Vivo, and Ex Vivo. *Chem. Sci.* **2019**, *10*, 7835−7851.
(13) Escorihuela, J.; Marcelis, A. T. M.; Zuilhof, H. Metal-Free Click Chemistry Reactions on Surfaces. *Adv. Mater. Interfaces* **2015**, *2*, 1500135−1500142.
(14) Blaszykowski, C.; Sheikh, S.; Thompson, M. Surface Chemistry to Minimize Fouling from Blood-Based Fluids. *Chem. Soc. Rev.* **2012**, *41*, 5599−5612.
(15) Tosatti, S.; De Paul, S. M.; Askendal, A.; VandeVondele, S.; Hubbell, J. A.; Tengvall, P.; Textor, M. Peptide Functionalized Poly(L-Lysine)-g-Poly(Ethylene Glycol) on Titanium: Resistance to Protein Adsorption in Full Heparinized Human Blood Plasma. *Biomaterials* **2003**, *24*, 4949−4958.
(16) Eeftens, J. M.; van der Torre, J.; Burnham, D. R.; Dekker, C. Copper-Free Click Chemistry for Attachment of Biomolecules in Magnetic Tweezers. *BMC Biophys.* **2015**, *8*, 1−7.
(17) Janissen, R.; Berghuis, B. A.; Dulin, D.; Wink, M.; Van Laar, T.; Dekker, N. H. Invincible DNA Tethers: Covalent DNA Anchoring for Enhanced Temporal and Force Stability in Magnetic Tweezers Experiments. *Nucleic Acids Res.* **2014**, *42*, No. e137.
(18) Kotagiri, N.; Li, Z.; Xu, X.; Mondal, S.; Nehorai, A.; Achilefu, S. Antibody Quantum Dot Conjugates Developed via Copper-Free Click Chemistry for Rapid Analysis of Biological Samples Using a Microfluidic Microsphere Array System. *Bioconjugate Chem.* **2014**, *25*, 1272−1281.
(19) Gunnarsson, A.; Jönsson, P.; Marie, R.; Tegenfeldt, J. O.; Höök, F. Single-Molecule Detection and Mismatch Discrimination of Unlabeled DNA Targets. *Nano Lett.* **2008**, *8*, 183−188.
(20) Jacob, A.; Van Ijzendoorn, L. J.; De Jong, A. M.; Prins, M. W. J. Quantification of Protein-Ligand Dissociation Kinetics in Heterogeneous Affinity Assays. *Anal. Chem.* **2012**, *84*, 9287−9294.
(21) Beyer, M. K. The Mechanical Strength of a Covalent Bond Calculated by Density Functional Theory. *J. Chem. Phys.* **2000**, *112*, 7307−7312.
(22) Michel, R.; Lussi, J. W.; Csucs, G.; Reviakine, I.; Danuser, G.; Ketterer, B.; Hubbell, J. A.; Textor, M.; Spencer, N. D. Selective Molecular Assembly Patterning: A New Approach to Micro- and Nanochemical Patterning of Surfaces for Biological Applications. *Langmuir* **2002**, *18*, 3281−3287.
(23) Wattendorf, U.; Kreft, O.; Textor, M.; Sukhorukov, G. B.; Merkle, H. P. Stable Stealth Function for Hollow Polyelectrolyte Microcapsules through a Poly(Ethylene Glycol) Grafted Polyelectrolyte Adlayer. *Biomacromolecules* **2008**, *9*, 100−108.
(24) Kenausis, G. L.; Vörös, J.; Elbert, D. L.; Huang, N.; Hofer, R.; Ruiz-Taylor, L.; Textor, M.; Hubbell, J. A.; Spencer, N. D. Poly(L-Lysine)-g-Poly(Ethylene Glycol) Layers on Metal Oxide Surfaces: Attachment Mechanism and Effects of Polymer Architecture on Resistance to Protein Adsorption. *J. Phys. Chem. B* **2000**, *104*, 3298−3309.
(25) Huang, N. P.; Michel, R.; Voros, J.; Textor, M.; Hofer, R.; Rossi, A.; Elbert, D. L.; Hubbell, J. A.; Spencer, N. D. Poly(L-Lysine)-g-Poly(Ethylene Glycol) Layers on Metal Oxide Surfaces: Surface-Analytical Characterization and Resistance to Serum and Fibrinogen Adsorption. *Langmuir* **2001**, *17*, 489−498.
(26) Weissgerber, T. L.; Milic, N. M.; Winham, S. J.; Garovic, V. D. Beyond Bar and Line Graphs: Time for a New Data Presentation Paradigm. *PLoS Biol.* **2015**, *13*, No. e1002128.
(27) Waikar, S. S.; Bonventre, J. V. Creatinine Kinetics and the Definition of Acute Kidney Injury. *J. Am. Soc. Nephrol.* **2009**, *20*, 672−679.

https://doi.org/10.1021/acssensors.1c00564
ACS Sens. 2021, 6, 1980−1986